Organic & Biomolecular Chemistry

This article is part of the

OBC 10th anniversary

themed issue

All articles in this issue will be gathered together online at

www.rsc.org/OBC10

Organic & Biomolecular Chemistry

www.rsc.org/obc

Volume 10 | Number 30 | 14 August 2012 | Pages 5661–6232

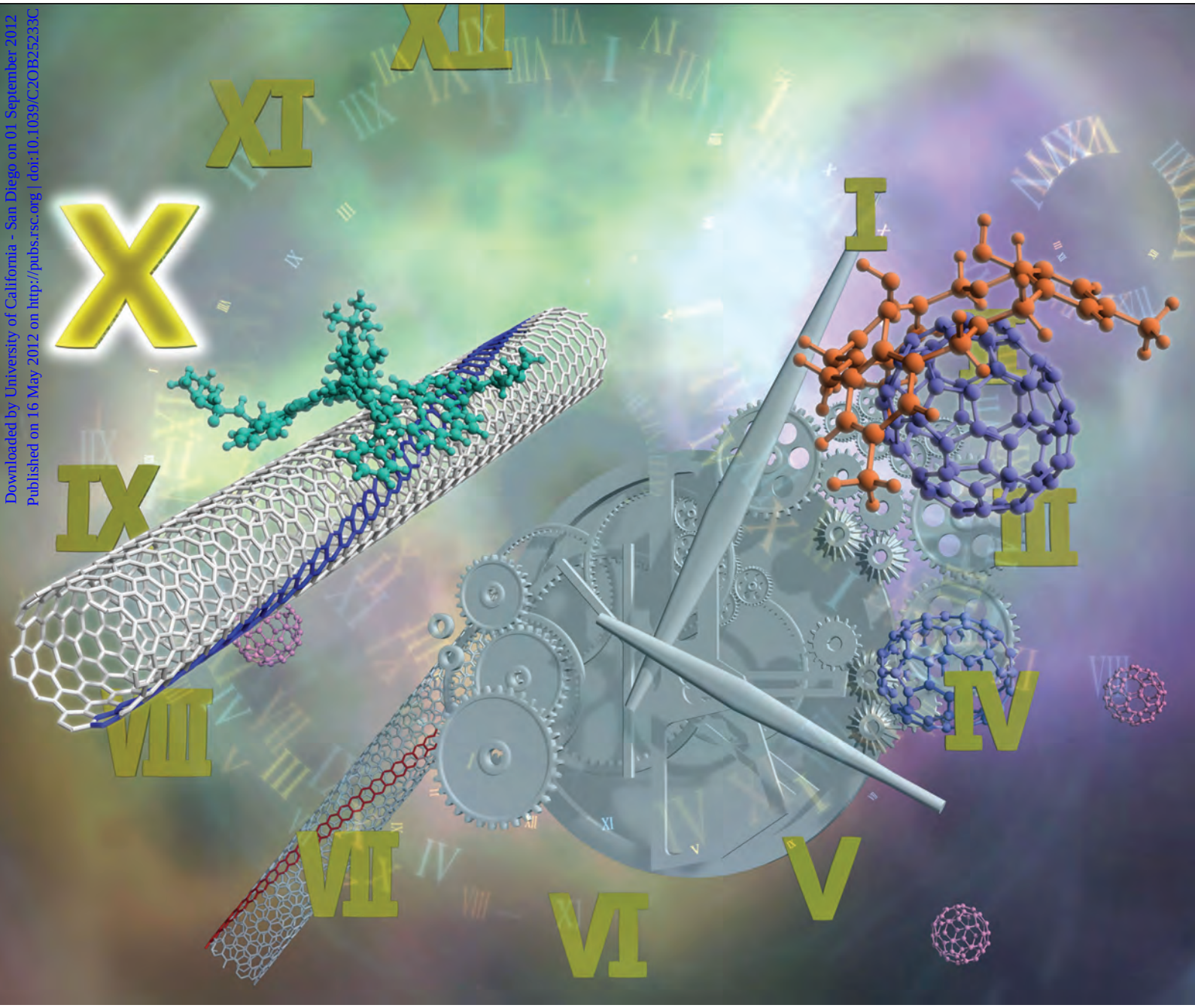

ISSN 1477-0520

RSC Publishing

FULL PAPER

Naoki Komatsu *et al.*

Preferential extraction of left- or right-handed single-walled carbon nanotubes by use of chiral diporphyrin nanotweezers

Organic & Biomolecular Chemistry

Dynamic Article Links
View Online

Cite this: *Org. Biomol. Chem.*, 2012, **10**, 5830

www.rsc.org/obc

PAPER

Preferential extraction of left- or right-handed single-walled carbon nanotubes by use of chiral diporphyrin nanotweezers†‡

Gang Liu,[a] Tatsuki Yasumitsu,[a,b] Li Zhao,[a] Xiaobin Peng,§[a] Feng Wang,¶[a] Ajoy K. Bauri,[c] Shuji Aonuma,[b] Takahide Kimura[a] and Naoki Komatsu*[a]

Received 1st February 2012, Accepted 30th April 2012
DOI: 10.1039/c2ob25233c

Handedness- and diameter-based separation of single-walled carbon nanotubes was achieved through preferential extraction of 76-CoMoCAT with 2,6-pyridylene-bridged chiral diporphyrin nanotweezers.

1. Introduction

A decade ago, an article entitled "Preferential precipitation of C_{70} over C_{60} with *p*-halohomooxacalix[3]arenes" was published in the first issue of *Organic & Biomolecular Chemistry*.[1] It was reported that C_{70} was precipitated from a mixture of C_{60} and C_{70} in toluene through preferential complexation with cyclic host molecules, namely *p*-halohomooxacalix[3]arenes.[2] In an opposite sense, insoluble single-walled carbon nanotubes (SWNTs) can be dissolved into an organic layer through preferential complexation with gable-type host molecules.[3] We extended the host–guest strategy from fullerenes to SWNTs[4] and realized their separation according to handedness and diameter by use of chiral diporphyrin nanotweezers.[5]

Since the electrical and optical properties of SWNTs are defined by their structures,[6] separation of SWNTs according to their structures has been attracting enormous interest in view of their applications. The following five kinds of methodology have been developed so far for their separation: electrophoresis, density gradient ultracentrifugation (DGU), chromatography, selective solubilisation, and selective reaction.[7,8] Separation of SWNTs through selective solubilisation was first reported by use of poly(phenylenevinylene) in 2000.[9] The polymer wrapping method, in particular by use of fluorene-based polymers, has been employed for isolation of SWNTs with a specific roll-up index, or (*n*,*m*).[7,10–12] Small molecules such as alkylamines were also used in separation of metallic and semiconducting SWNTs through selective solubilisation.[13,14] Recently, tailored host molecules have attracted increasing attention, because the specific structure in SWNTs can be targeted rationally.[15–19] In fact, rationally designed chiral nanotweezers discriminated the diameters and the handedness of SWNTs simultaneously to enrich the enantiomers of (6,5)- and (7,6)-SWNTs.[20–24] However, (*n*,*m*)-SWNTs optically enriched by our method have been limited mainly to (6,5)- and (7,6)-SWNTs.[7,10–12] Herein, we report on enantiomeric enrichment of other (*n*,*m*)-SWNTs,[25–27] such as (8,4)- and (9,1)-SWNTs, than the so far reported ones[5,20,21,23,28] together with simultaneous separation according to their diameters through preferential extraction of commercial SWNTs (76-CoMoCAT) with 2,6-pyridylene-bridged chiral diporphyrin nanotweezers.[28]

2. Results and discussion

2.1. Helical chirality in SWNTs

Although most of the chiral molecules possess stereogenic centres, the molecules without stereogenic centres may have axial chirality. Helical chirality, or helicity, is one kind of axial chirality and indicates left- and right-handed mirror image structures. All the SWNTs other than zigzag and armchair possess helical chirality defined as *M* and *P* shown in Fig. 1.[7,8,22] A helical structure of SWNT is different from those of the materials known so far. The α-Helix, occurring in many proteins, and DNA form a spring-shaped helix connected by amide and phosphate ester linkages, respectively. Helicene fabricates a stair-like helix consisting of annulated aromatic rings. On the other hand, a chiral SWNT is constructed with a tubular-shaped helix depicted in Fig. 1. These three types of helical chirality are illustrated in Fig. 2. The helical tube structure in SWNTs is more rigid than other types of helices, because it is rigorously fixed by

[a]*Department of Chemistry, Shiga University of Medical Science, Seta, Otsu 520-2192, Japan. E-mail: nkomatsu@belle.shiga-med.ac.jp; Fax: +81-77-548-2405; Tel: +81-77-548-2102*
[b]*Department of Applied Chemistry, Osaka Electro-Communication University, Neyagawa, Osaka 572-8530, Japan*
[c]*Bio-Organic Division, Bhabha Atomic Research Center, Trombay, Mumbai 400085, India*

†This article is part of the *Organic & Biomolecular Chemistry* 10th Anniversary issue.

‡Electronic supplementary information (ESI) available: Deconvoluted CD peaks (Fig. S1). See DOI: 10.1039/c2ob25233c

§Present address: Institute of Polymer Optoelectronic Materials and Devices, State Key Laboratory of Luminescent Materials and Devices, South China University of Technology, Guangzhou 510640, China.
¶Present address: Key Laboratory for Green Chemical Process of Ministry of Education, Wuhan Institute of Technology, Wuhan 430073, China.

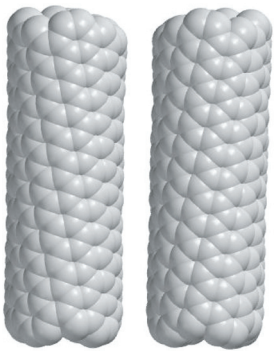

Fig. 1 Helical chirality of (*M*)- and (*P*)-(8,4)-SWNTs (left and right images, respectively).

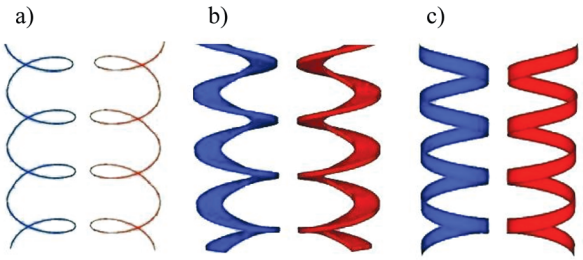

Fig. 2 Schematic representation of spring-shaped (a), stair-like (b), and tubular-shaped (c) helices with left-and right-handed structures.

covalent bonds. SWNTs are considered to be a new type of helical material in terms of the structure and rigidity.

2.2. Molecular design in nanotweezers

The nanotweezers consist of two porphyrin legs and a rigid bridge connecting them (Chart 1). Since porphyrin is known to have strong affinity to the widely expanded curved π-conjugation system,[3] the cavity made by the two porphyrins in the nanotweezers can accept a SWNT to form a complex. However, the size and shape of the accepted SWNT should match those of the cavity in the nanotweezers to form a stable complex. Since the nanotweezers are soluble in organic solvent, the only SWNTs capable of forming stable complexes with the nanotweezers can be extracted in an organic layer. Therefore, we can rationally design the nanotweezers having an appropriate cavity by tuning the angle and the distance of the two porphyrin units for extracting the specific diameter of SWNTs preferentially. In addition, one more function can be given to the nanotweezers; that is, the stereogenic centres at the periphery of the porphyrins can discriminate the handedness of chiral SWNTs, providing optical activity to SWNTs. The chiral diporphyrin nanotweezers can recognize diameter and handedness simultaneously.

When the chiral nanotweezers **1** was applied to the extraction of 65-CoMoCAT (SWNTs prepared by a chemical vapor deposition (CVD) process using a silica-supported Co–Mo catalyst),[29] (6,5)-SWNTs were found to be optically enriched much more than other SWNTs included in 65-CoMoCAT. We also found that SWNTs with relatively small roll-up angles, such as (8,3)-, (8,4)-, and (9,4)-SWNTs, were enriched in their

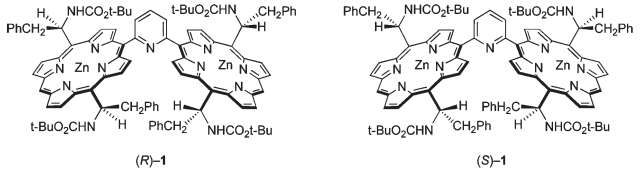

Chart 1 Structures of chiral diporphyrin nanotweezers, (*R*)- and (*S*)-**1**.

abundance after the extraction.[28] Although (6,5)-SWNTs, one of the main components in 65-CoMoCAT, decreased in their abundance, they were still included in significant amounts in the extract, meaning that the abundance of the enriched SWNTs was not so high in the extract. Since 76-CoMoCAT has a wider range of roll-up angles (5.2–27.5°) and includes a higher rate of SWNTs with larger diameters (0.84–0.92 nm) than 65-CoMoCAT, we expected different selectivity of the nanotweezers **1** toward 76-CoMoCAT and employed it for the extraction of 76-CoMoCAT. As a result, a large increase was found in the abundance of SWNTs with relatively large diameters and in the optical purity of some SWNTs other than (6,5)-SWNTs, which will be discussed in the sections of 2.4 and 2.5, respectively.

2.3. Extraction of SWNTs with nanotweezers

After a mixture of 76-CoMoCAT and **1** in methanol was bath-sonicated, the resulting black suspension was centrifuged to obtain the homogeneous supernatant as an extract. The absorption and circular dichroism (CD) spectra of the extract are shown in Fig. 3. The large upward shift of the baseline, and the red shift and broadening of the Soret and Q bands in the absorption spectra indicate that a significant amount of SWNTs exists as complexes with nanotweezers in the extract (Fig. 3a). A different degree of the baseline shift of the extracts with (*R*)- and (*S*)-**1** indicates that the amounts of the extracted SWNTs are different under the same extraction conditions. This is considered to be caused by not stereoisomerism, but just experimental error. Broad peaks originating from the extracted SWNTs are clearly observed in the E^{S}_{11} region (850–1300 nm, electronic transition parallel to the nanotube axis in semiconducting SWNTs).

In the CD spectra shown in Fig. 3b, the chiral diporphyrins, (*R*)- and (*S*)-**1**, exhibit symmetrical bisignate Cotton effects at 409 and 419 nm in the Soret band. In the extracts, they shift to the longer wavelengths at 434 and 452 nm, and their intensity increases significantly. The red shifts in the CD spectra of the extracts are consistent with that in the absorption spectra mentioned above. The CD enhancement can be attributed to the fixation of the asymmetric conformation in diporphyrins on the surface of the SWNTs as shown in Fig. 4.[30] The spectral change in CD supports the above conclusion of the dissolvation of the SWNT complex with chiral nanotweezers in the extract.

2.4. (*n*,*m*) Enrichment through extraction

After the methanol extracts of 76-CoMoCAT with (*R*)- and (*S*)-**1** were concentrated, the resulting black solids were washed with THF and pyridine several times to wash out the nanotweezers from the complex. More than 70% of the chiral nanotweezers

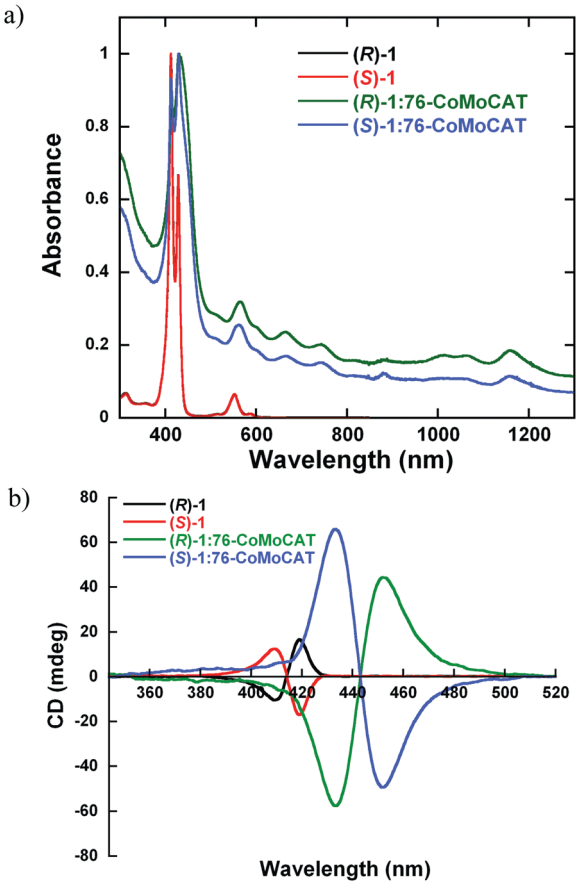

Fig. 3 (a) Absorption spectra of (*R*)- and (*S*)-**1** before and after extraction of 76-CoMoCAT. (b) CD spectra of (*R*)- and (*S*)-**1** before and after extraction of 76-CoMoCAT. CD spectra were normalized at the absorbance of 429 nm in the absorption spectra.

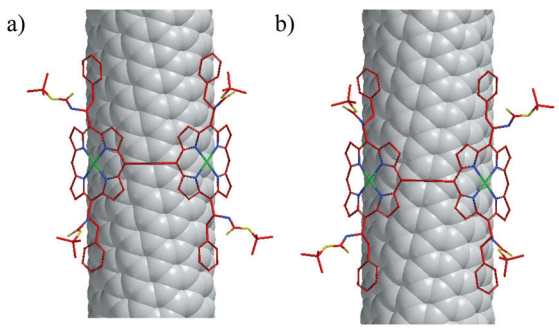

Fig. 4 Computer-generated complex structures of (*R*)-**1**: (*M*)-(8,4)-SWNT (a) and (*S*)-**1**: (*P*)-(8,4)-SWNT (b).

were recovered and reused after purification. The washed SWNTs were dissolved in D_2O in the presence of achiral detergent, sodium dodecylbenzenesulfonate (SDBS), for spectroscopic measurements of photoluminescence (PL), absorption, and CD.[31]

In the PL spectra, the content of (7,5)- and (6,5)-SWNTs, the two main components in 76-CoMoCAT, significantly decreases as shown in Fig. 5. The PL from (6,5)-SWNTs almost disappears after the extraction. The abundance of (8,3)-SWNTs is also shown to decrease in the PL. Instead, the abundance of (8,4)-, (9,4)-, (10,2)-, and (7,6)-SWNTs increases significantly. Although (9,4)- and (10,2)-SWNTs are trace constituents in 76-CoMoCAT before extraction, they become major components after the extraction.

(*n*,*m*)-SWNTs increased and decreased through the extraction are almost consistent with those in the case of 65-CoMoCAT, where the abundance of (6,4)-, (6,5)-, and (7,5)-SWNTs decreased and that of (8,3)-, (8,4)-, and (9,4)-SWNTs increased.[28] However, (8,3)-SWNTs increase and decrease in their abundance in the cases of 65- and 76-CoMoCAT, respectively. Because of a slight difference at the PL before and after the extraction, the opposite behavior of (8,3)-SWNTs may be caused by a small difference in the conditions of the extraction of 65- and 76-CoMoCAT: amounts of the nanotweezers and SWNTs, and volume of methanol. The preference of the nanotweezers **1** toward (*n*,*m*) can be seen more clearly in the extraction of 76-CoMoCAT than 65-CoMoCAT.[28] This is probably because these preferentially extracted SWNTs included in 76-CoMoCAT have appropriate diameters for the cavity of **1**, while the diameters of SWNTs in 65-CoMoCAT are smaller than the size of the cavity.

In order to quantify the change in the PL intensity, we calculated the abundance of the nine components in 76-CoMoCAT clearly detected in the PL spectra shown in Fig. 5. The results are summarised in Table 1. Because the difference in the quantum yield and absorption coefficient is not reflected in the calculations, the abundance in Table 1 is not the actual one, but an estimated one. Since stereoisomers, (*R*)- and (*S*)-**1**, should give the same (*n*,*m*) abundance of the extracted SWNTs theoretically, the difference observed in Table 1 can be attributed to experimental error caused probably by a difference in the degree of bundling. Although 60% of the abundance is occupied by (6,5)-, (8,3)-, and (7,5)-SWNTs in 76-CoMoCAT, the abundance decreases significantly to 18% or less after the extraction with **1**. On the other hand, the abundance of (9,4)-SWNTs increases by more than double from 7% to over 19%. Among the rest of the components in 76-CoMoCAT, (8,4)-, (10,2)-, and (7,6)-SWNTs also increase significantly in their abundance after the extraction. Although the abundance of (8,6)-SWNTs slightly increases, the abundant (*n*,*m*) is drastically changed from (6,5), (8,3), and (7,5) to (8,4), (10,2), (7,6), and (9,4) as illustrated in Fig. 6. The significantly enriched SWNTs, (8,4)-, (10,2)-, (7,6)-, and (9,4)-SWNTs, have larger diameters (0.84–0.92 nm) and a wider range of roll-up angles (9.0–27.5°) than the components decreased in abundance after the extraction, (6,5)-, (8,3)-, and (7,5)-SWNTs (0.76–0.83 nm, 15.3–27.0°). This clearly indicates that the nanotweezers **1** discriminates the diameters of SWNTs rather than the roll-up angles.

Drastic change is also observed in absorption spectra through the extraction, especially in the E^{S}_{11} region (Fig. 7). The absorbance corresponding to the two main components in 76-CoMoCAT, (6,5)- and (7,5)-SWNTs, at 980 and 1024 nm decreases significantly after the extraction, which is consistent with the above-mentioned result of the PL (Fig. 5 and Table 1). On the other hand, the peak at 1113 nm corresponding to (9,4)-, (8,4)-, and (7,6)-SWNTs becomes dominant after the extraction. This phenomenon can be interpreted by the abundance (%) estimated from the PL (Table 1); that is, the abundance of (9,4)-,

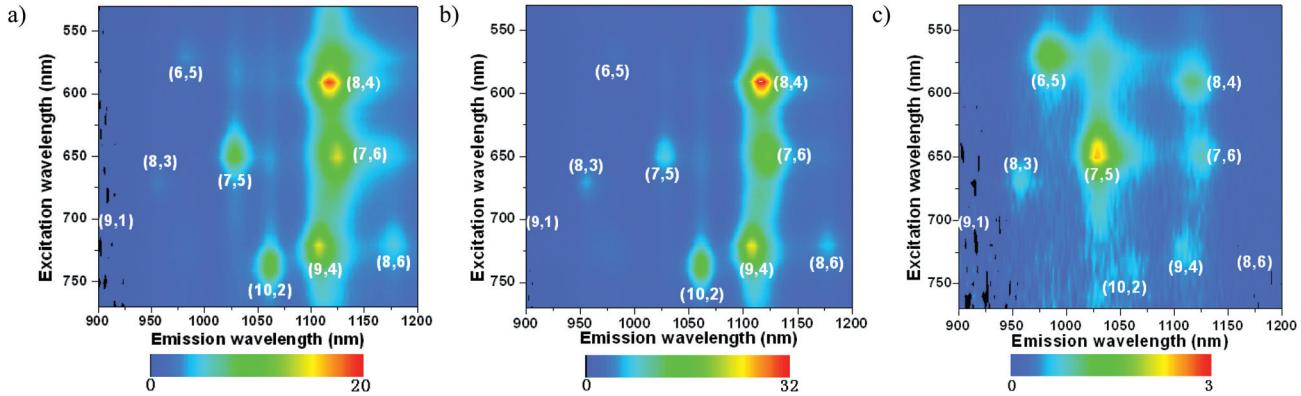

Fig. 5 PL spectra of 76-CoMoCAT after extraction with (*R*)-**1** (a) and (*S*)-**1** (b), and before extraction (c). The intensity scales are shown below the spectra.

Table 1 (*n*,*m*) Abundance of semiconducting SWNTs before and after extraction of 76-CoMoCAT with (*R*)- and (*S*)-**1**[a]

			Abundance (%) estimated from PL spectra						
(*n*,*m*) Components in 76-CoMoCAT	Diameter (nm)	Roll-up angle (°)	76-CoMoCAT[b]	Extraction with (*R*)-**1**[c]	Extraction with (*S*)-**1**[d]	λ_{11} [e] (nm)	λ_{22} [e] (nm)	λ_{33} [e] (nm)	λ_{44} [e] (nm)
(9,1)	0.76	5.2	2	0	0	912	691	—	—
(6,5)	0.76	27.0	20	4	3	976	566	345	300
(8,3)	0.78	15.3	10	3	5	952	665	353	309
(7,5)	0.83	24.5	30	11	7	1024	645	336	288
(8,4)	0.84	19.1	13	25	29	1111	589	384[f]	—
(10,2)	0.88	9.0	6	13	14	1053	737	372	316
(7,6)	0.90	27.5	10	19	16	1120	648	371	320
(9,4)	0.92	17.5	7	19	21	1101	722	360	341
(8,6)	0.97	25.3	2	6	5	1173	718	390	350

[a] The abundance is calculated on the basis of the fluorescence intensity in Fig. 5. [b] Fig. 5c. [c] Fig. 5a. [d] Fig. 5b. [e] Ref. 33. [f] Ref. 26.

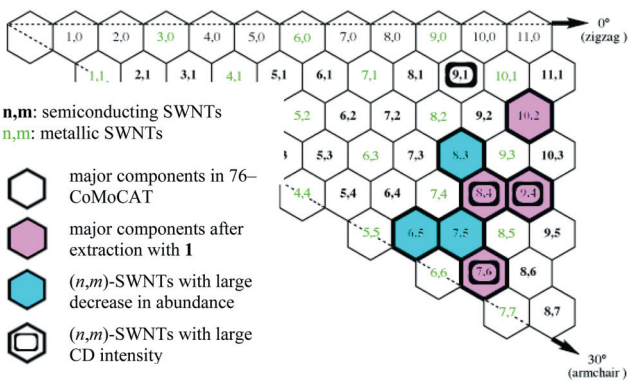

Fig. 6 Summary of abundant and optically active (*n*,*m*)-SWNTs through the extraction of 76-CoMoCAT with **1**.

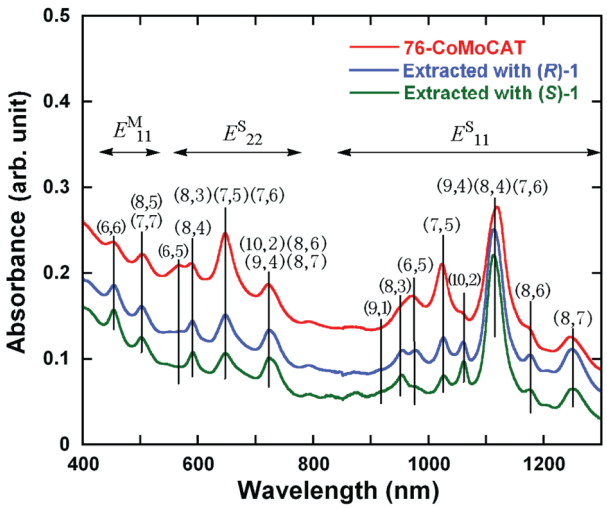

Fig. 7 Absorption spectra of 76-CoMoCAT before and after extraction with (*R*)- and (*S*)-**1**.

(8,4)-, and (7,6)-SWNTs amounts to around 65% from 30% through the extraction with **1**. Increase of (10,2)-SWNTs is also confirmed at 1060 nm, while decrease of (8,3)-SWNTs is not observed as clearly as that in PL (Fig. 5 and Table 1). The absorption at longer wavelength corresponding to (8,6)- and (8,7)-SWNTs increases slightly in Fig. 7. These results in the absorption spectra support the conclusion drawn from the PL spectra (Fig. 5 and Table 1); (8,4)-, (10,2)-, (7,6)-, and (9,4)-

SWNTs with diameters of 0.84–0.92 nm are the major components in the extract through large enrichment, while smaller diameters significantly decrease and larger diameters slightly increase through the extraction (Fig. 6).

Since the four main components in the extract are distributed to the three peaks at 590, 648, and 724 nm in the E^{S}_{22} region (550–750 nm) in Fig. 7, the change in the peak intensity through the extraction in this region is not so prominent as that in the E^{S}_{11} region discussed above. However, it is shown that the peak of (6,5)-SWNTs at 569 nm almost disappears, and the peak at 648 nm including (7,5)-SWNTs becomes smaller after the extraction.

As for metallic SWNTs, the absorption corresponding to (6,6) at 455 nm, and (8,5) and/or (7,7) at 507 nm is observed in the E^{M}_{11} region (Fig. 7).[32] The relative intensity of these two peaks does not change so much before and after the extraction, indicating that the nanotweezers **1** was not able to discriminate these metallic SWNTs. In addition, no marked difference is observed in the ratio between the absorption of the metallic and semiconducting SWNTs before and after the extraction. That is, the extraction with the nanotweezers **1** does not affect the ratio between the metallic and semiconducting SWNTs, indicating that **1** did not recognise the metallicity of SWNTs.

2.5. Optical enrichment through extraction

Separation of SWNTs according to the handedness is confirmed by CD of the SDBS–D_2O solutions of the washed SWNTs after the extraction. The SWNTs extracted with chiral nanotweezers, (*R*)- and (*S*)-**1**, exhibit symmetrical CDs as shown in Fig. 8, indicating that the extracted SWNTs are optically active. The four prominent peaks observed in the E^{S}_{22} region mean that the solutions include at least four kinds of optically active (*n*,*m*)-SWNTs. These peaks are assigned as indicated in Fig. 8 by taking into account the reported absorption wavelength of the major components of 76-CoMoCAT summarised in Table 1.[26,33] Deconvolution of the four peaks shown in Fig. S1‡ indicates that each peak consists of one main component with a small contribution from other SWNTs. The peaks at 588 and 691 nm are assigned as (8,4)- and (9,1)-SWNTs, respectively, because no other SWNTs in the major components of 76-CoMoCAT exhibit absorption near the above wavelengths in the E^{S}_{22} region (Table 1). Additional small peaks at 916 nm with their signs opposite to those at 691 nm are detected probably due to λ_{11} of (9,1)-SWNTs. Although the peaks at 649 nm are close to the reported wavelengths of (8,3)-, (7,5)-, and (7,6)-SWNTs, they are assigned as (7,6)-SWNTs. This is because the observed wavelength (649 nm) is closest to the reported one for (7,6)-SWNTs (648 nm), and the CDs corresponding to (8,3)- and (7,5)-SWNTs are not observed in the E^{S}_{11} region (Table 1). The peaks at 720 nm are very close to the reported wavelengths of (9,4)- and (8,6)-SWNTs (722 and 718 nm, respectively) among the four candidates, (10,2)-, (8,7)-, (9,4)- and (8,6)-SWNTs. Taking the much larger abundance shown in Table 1 into consideration, (9,4)-SWNTs are more probable than (8,6)-SWNTs for the peaks at 720 nm. However, (8,6)-SWNTs are still conceivable because of a lack of strong evidence in the E^{S}_{11} and E^{S}_{33} regions. Since many SWNTs have absorption at 300–400 nm as shown in Table 1, it is difficult for us to use the CDs in E^{S}_{33} and E^{S}_{44} regions to assign the peaks.

Among the major components in the extracted SWNTs, (8,4)-SWNTs exhibit the strongest CD intensity at 588 nm. (9,4)- and (7,6)-SWNTs also give the relatively large CDs at 720 and 649 nm, respectively, whose signs are opposite to that of (8,4)-SWNTs. The CD intensity of (8,4)-, (9,4)-, and (7,6)-SWNTs qualitatively correlates with their abundance discussed in the preceding section (Table 1), implying that (8,4)-, (9,4)-, and (7,6)-SWNTs possess similar enantiomeric excess (ee) and each pair of the enantiomers has a similar degree of difference in extinction coefficients for left and right circularly polarised light. While (8,4)-, (9,4)-, and (7,6)-SWNTs are optically enriched through the extraction with (*R*)- and (*S*)-**1**, no clear CD is observed at the wavelengths of 737 and 1053 nm (Fig. 8 and S1‡) corresponding to (10,2)-SWNTs with the fourth largest abundance in the extract estimated from the PL spectra (Fig. 5 and Table 1). That is, (10,2)-SWNTs are enriched in the abundance, but not in the optical activity through the extraction, indicating that the nanotweezers **1** recognises diameter and handedness of SWNTs independently. An opposite phenomenon observed in the case of (9,1)-SWNTs supports the conclusion of

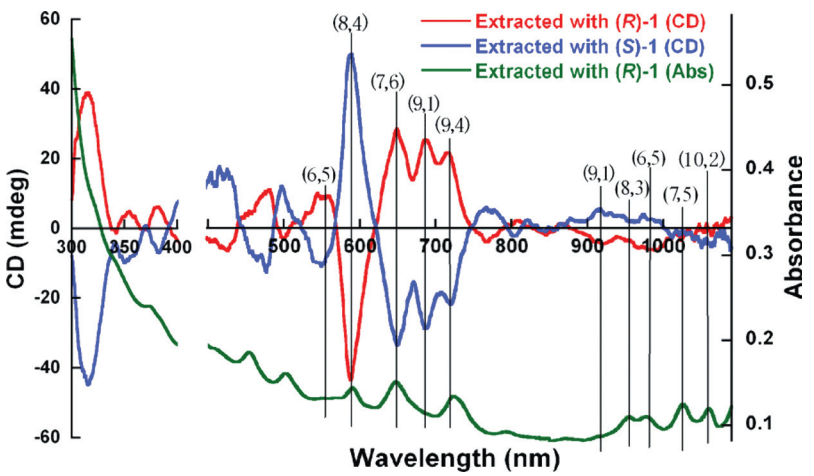

Fig. 8 CD spectra of SWNTs extracted with (*R*)- and (*S*)-**1**, and absorption spectra of SWNTs extracted with (*R*)-**1**. CD spectra were normalized at the absorption at 1113 nm. The spectra at 300–400 nm and 400–1100 nm were taken using different spectropolarimeters.

independent recognition; although no clear PL and only tiny absorption are detected for (9,1)-SWNTs at 691 and 912 nm shown in Fig. 5 and 7, the CD of (9,1)-SWNTs at 691 nm has comparable intensity with those of (9,4)-, and (7,6)-SWNTs as shown in Fig. 8. This may imply that the nanotweezers **1** discriminates handedness of (9,1)-SWNTs more strictly than the diameter, resulting in the small abundance with high ee of (9,1)-SWNTs. However, another possibility is that the enantiomers of (9,1)-SWNTs have a much larger difference in extinction coefficients for left and right circularly polarised light than (8,4)-, (9,4)-, and (7,6)-SWNTs, giving the CD intensity comparable with those of the abundant SWNTs regardless of the abundance and the ee of the extracted (9,1)-SWNTs.

SWNTs exhibiting relatively large CD intensity are shown in the map (Fig. 6). After the extraction of 65-CoMoCAT with **1** reported previously,[28] (6,5)-SWNTs were still included in significant amounts as one of the major components in the extract, although they were decreased in their abundance through the extraction. Only (6,5)-SWNTs exhibited prominent CDs under these circumstances. On the other hand, the SWNTs extracted from 76-CoMoCAT exhibit CDs corresponding to (8,4)-, (7,6)-, (9,1)-, and (9,4)-SWNTs rather than (6,5)-SWNTs as shown in Fig. 8. The discrepancy between 65- and 76-CoMoCAT may arise from large differences in the abundance of (6,5)-SWNTs in these extracts.

3. Concluding remarks

In 2007, we published a paper about the first experimental example of optically active SWNTs, which were obtained through optical resolution by use of the chiral nanotweezers.[5] The unique methodology to separate the handedness of SWNTs is based on the idea of preferential precipitation of C_{70} from a toluene solution of C_{60} and C_{70}.[1] Tweezer-shaped host molecules were designed for a tubular-shaped guest, as circular-shaped host molecules were employed for the recognition of spherical fullerenes. Insoluble SWNTs were intended to be soluble through complexation with the nanotweezers, as soluble C_{70} was precipitated out from the solution through complexation with the calixarenes. Since then, we have developed the molecular design of the nanotweezers by changing the aromatic bridge[20,21,23,28] and the two legs[15] to improve the selectivities for diameters and/or handedness of SWNTs. Here, we reported on optical enrichment of SWNTs with (*n*,*m*) other than the so far reported ones in addition to the selectivity to the relatively large diameters with narrow range.

As summarized in Fig. 6, (8,4)-, (10,2)-, (7,6)-, and (9,4)-SWNTs became the major components in the extract, while the abundance of the major components in 76-CoMoCAT, (7,5)-, (8,3)-, and (6,5)-SWNTs, decreased significantly. This indicates that the nanotweezers **1** recognized diameters of SWNTs and selectively extracted SWNTs with relatively large diameters of 0.84–0.92 nm rather than smaller ones of 0.76–0.83 nm. Since the nanotweezers are considered to discriminate the diameter and handedness independently, not all the major components in the extract exhibit large CDs; (8,4)-, (9,4)-, and (7,6)-SWNTs show relatively large CDs, while almost no CD is observed in (10,2)-SWNTs. It is noteworthy that (9,1)-SWNTs show CD intensity comparable to those of (8,4)-, (9,4)-, and (7,6)-SWNTs in spite of the trace component.

Next to the fullerenes and CNTs, we separated highly soluble nanodiamond by chromatography in view of biomedical application.[34] We believe that we can report more fascinating results on the chemistry of nanocarbons.

4. Experimental

Materials

SWNTs (SWeNT SG76, designated as 76-CoMoCAT in this paper, Lot No. MKBC9978) were purchased from Sigma-Aldrich Co. All the reagents were obtained from Sigma-Aldrich Co., Wako Pure Chemical Industries, Ltd, Nacalai Tesque, Inc., and Tokyo Chemical Industry Co., Ltd, and were used as received. The chiral diporphyrin nanotweezers, (*R*)- and (*S*)-**1**, were synthesised through the Suzuki–Miyaura coupling reaction between chiral porphyrin boronate and 2,6-dibromopyridine according to our previous report.[28]

Equipment

UV-vis-NIR absorption spectra were obtained on a UV-3100PC scanning spectrophotometer (Shimadzu Co.). PL spectra were measured on a NIR-PL system (Shimadzu Co.). CD spectra were recorded on J-600 and J-820 spectropolarimeters (JASCO International Co. Ltd). Centrifugation was carried out with Avanti J-E and Optima-TL (Beckman Coulter, Inc.). Tip-sonication was performed with MISONIX (110 W, 20 kHz).

Extraction of 76-CoMoCAT with chiral nanotweezers 1

Chiral nanotweezers (*R*)- or (*S*)-**1** (7.0 mg) and 76-CoMoCAT (10.5 mg) in methanol (40 mL) were bath-sonicated at 20 °C for 7 h. After centrifugation of the resulting suspension at 50 400 *g* for 5 h, the homogeneous supernatant was subjected to UV-vis-NIR and CD measurements (Fig. 3a and b, respectively). After concentration, the residue was washed with THF and pyridine several times until the porphyrin Soret band disappeared in the UV-vis spectra of the washings. An aliquot (0.1 mg) of the washed SWNTs was dispersed in D_2O (10 mL) in the presence of SDBS (1.0 mg mL^{-1}) by sonication for 40 min with tip-type apparatus. After ultracentrifugation of the resulting suspension at 347 000 *g* for 40 min, the upper layer (~75%) of the supernatant was subjected to PL, UV-vis-NIR, and CD measurements (Fig. 5, 7, and 8, respectively).

Acknowledgements

The authors would like to thank Prof. Hiroshi Imahori, Dr Tomokazu Umeyama, and Dr Tatsuya Murakami (Kyoto University), and Prof. Yasushi Kawai (Nagahama Institute of Bio-Science and Technology) for allowing us to use the PL spectrophotometer and the CD spectropolarimeter, respectively. We are grateful to Mr Tomohiro Shimonishi and Ms Yoshimi Shibata (JASCO Co.) for manipulating the CD data. FW acknowledges the financial support from Natural Science Foundation of China

(Grant No. 51103111). This work was financially supported by Grant-in-Aid for Scientific Research on Priority Areas (No. 22016005), Grant-in-Aid for Scientific Research (B) (No. 23350062), the Kurata Memorial Hitachi Science and Technology Foundation, Adaptable and Seamless Technology Transfer Program through Target-driven R&D (JST), and Industrial Technology Research Grant Program in 2005 from New Energy and Industrial Technology Development Organisation (NEDO) of Japan.

Notes and references

1 N. Komatsu, *Org. Biomol. Chem.*, 2003, **1**, 204–209.
2 N. Komatsu, *Tetrahedron Lett.*, 2001, **42**, 1733–1736.
3 N. Komatsu, in *Topics in Heterocyclic Chemistry*, ed. K. Matsumoto, Springer, Heidelberg, 2008, pp. 161–198.
4 N. Komatsu, *J. Inclusion Phenom. Macrocyclic Chem.*, 2008, **61**, 195–216.
5 X. Peng, N. Komatsu, S. Bhattacharya, T. Shimawaki, S. Aonuma, T. Kimura and A. Osuka, *Nat. Nanotechnol.*, 2007, **2**, 361–365.
6 H. Kataura, Y. Kumazawa, Y. Maniwa, I. Umezu, S. Suzuki, Y. Ohtsuka and Y. Achiba, *Synth. Met.*, 1999, **103**, 2555–2558.
7 G. Liu, F. Wang, X. Peng, A. F. M. M. Rahman, A. K. Bauri and N. Komatsu, in *Handbook of Carbon Nano Materials*, ed. F. D'Souza and K. M. Kadish, World Scientific, 2012, vol. 3, pp. 203–232.
8 N. Komatsu and F. Wang, *Materials*, 2010, **3**, 3818–3844.
9 A. B. Dalton, C. Stephan, J. N. Coleman, B. McCarthy, P. M. Ajayan, S. Lefrant, P. Bernier, W. J. Blau and H. J. Byrne, *J. Phys. Chem. B*, 2000, **104**, 10012–10016.
10 H. Ozawa, N. Ide, T. Fujigaya, Y. Niidome and N. Nakashima, *Chem. Lett.*, 2011, **40**, 239–241.
11 F. Lemasson, J. Tittmann, F. Hennrich, N. Stürzl, S. Malik, M. M. Kappes and M. Mayor, *Chem. Commun.*, 2011, **47**, 7428–7430.
12 A. Nish, J.-Y. Hwang, J. Doig and R. J. Nicholas, *Nat. Nanotechnol.*, 2007, **2**, 640–646.
13 Y. Maeda, S. Kimura, M. Kanda, Y. Hirashima, T. Hasegawa, T. Wakahara, Y. Lian, T. Nakahodo, T. Tsuchiya, T. Akasaka, J. Lu, X. Zhang, Z. Gao, Y. Yu, S. Nagase, S. Kazaoui, N. Minami, T. Shimizu, H. Tokumoto and R. Saito, *J. Am. Chem. Soc.*, 2005, **127**, 10287–10290.
14 D. Chattopadhyay, I. Galeska and F. Papadimitrakopoulos, *J. Am. Chem. Soc.*, 2003, **125**, 3370–3375.
15 A. F. M. M. Rahman, F. Wang, K. Matsuda, T. Kimura and N. Komatsu, *Chem. Sci.*, 2011, **2**, 862–867.
16 C. Backes, F. Hauke and A. Hirsch, *Adv. Mater.*, 2011, **23**, 2588–2601.
17 C. Backes, C. D. Schmidt, F. Hauke and A. Hirsch, *Chem. Asian J.*, 2011, **6**, 438–444.
18 R. Marquis, K. Kulikiewicz, S. Lebedkin, M. M. Kappes, C. Mioskowski, S. Meunier and A. Wagner, *Chem.–Eur. J*, 2009, **15**, 11187–11196.
19 R. M. Tromp, A. Afzali, M. Freitag, D. B. Mitzi and Z. Chen, *Nano Lett.*, 2008, **8**, 469–472.
20 F. Wang, K. Matsuda, A. F. M. M. Rahman, T. Kimura and N. Komatsu, *Nanoscale*, 2011, **3**, 4117–4124.
21 F. Wang, K. Matsuda, A. F. M. M. Rahman, X. Peng, T. Kimura and N. Komatsu, *J. Am. Chem. Soc.*, 2010, **132**, 10876–10881.
22 X. Peng, F. Wang, A. K. Bauri, A. F. M. M. Rahman and N. Komatsu, *Chem. Lett.*, 2010, **39**, 1022–1027.
23 X. Peng, N. Komatsu, T. Kimura and A. Osuka, *ACS Nano*, 2008, **2**, 2045–2050.
24 E. M. Pérez and N. Martin, *Org. Biomol. Chem.*, 2012, **10**, 3577–3583.
25 A. A. Green and M. C. Hersam, *Adv. Mater.*, 2011, **23**, 2185–2190.
26 S. Ghosh, S. M. Bachilo and R. B. Weisman, *Nat. Nanotechnol.*, 2010, **5**, 443–450.
27 A. A. Green, M. C. Duch and M. C. Hersam, *Nano Res.*, 2009, **2**, 69–77.
28 X. Peng, N. Komatsu, T. Kimura and A. Osuka, *J. Am. Chem. Soc.*, 2007, **129**, 15947–15953.
29 S. M. Bachilo, L. Balzano, J. E. Herrera, F. Pompeo, D. E. Resasco and R. B. Weisman, *J. Am. Chem. Soc.*, 2003, **125**, 11186–11187.
30 V. V. Borovkov, G. A. Hembury and Y. Inoue, *Acc. Chem. Res.*, 2004, **37**, 449–459.
31 S. M. Bachilo, M. S. Strano, C. Kittrell, R. H. Hauge, R. E. Smalley and R. B. Weisman, *Science*, 2002, **298**, 2361–2366.
32 A. Jorio, A. P. Santos, H. B. Ribeiro, C. Fantini, M. Souza, J. P. M. Vieira, C. A. Furtado, J. Jiang, R. Saito, L. Balzano, D. E. Resasco and M. A. Piementa, *Phys. Rev. B*, 2005, **72**, 075207.
33 R. B. Weisman and S. M. Bachilo, *Nano Lett.*, 2003, **3**, 1235–1238.
34 L. Zhao, T. Takimoto, M. Ito, N. Kitagawa, T. Kimura and N. Komatsu, *Angew. Chem., Int. Ed.*, 2011, **50**, 1388–1392.

